

**VIBRO-ACOUSTIC DESIGN OF AN AIRCRAFT-TYPE
ACTIVE WINDOW. PART 1: DYNAMIC MODELLING AND
EXPERIMENTAL VALIDATION**

IGNAZIO DIMINO

*CIRA, The Italian Aerospace Research Centre, Vibro-Acoustics and Smart Structures Laboratory,
Capua, Italy and PhD Student at Imperial College London, Department of Aeronautics, London,
Great Britain; e-mail: i.dimino@cira.it*

ANDREA VIGLIOTTI

*CIRA, The Italian Aerospace Research Centre, Vibro-Acoustics and Smart Structures Laboratory,
Capua, Italy; e-mail: a.vigliotti@cira.it*

M.H. FERRI ALIABADI

*Imperial College London, Department of Aeronautics, London, Great Britain;
e-mail: m.h.aliabadi@imperial.uk*

ANTONIO CONCILIO

*CIRA, The Italian Aerospace Research Centre, Vibro-Acoustics and Smart Structures Laboratory,
Capua, Italy; e-mail: a.concilio@cira.it*

Recent investigations show that active noise control methods can improve noise reduction capabilities of aircraft-type windows in the low-frequency region. Being a privileged path for external noise transmission and one of the main causes of high interior noise levels in a treated aircraft, a proper design of the aircraft window can significantly contribute to the reduction of cabin noise levels with a minimum impact on the aircraft mass and performances. This is the first part of two companion papers. In this paper (Part 1), the vibro-acoustic design of a triple-pane aircraft-type window prototype is presented. Numerical and experimental activities addressing the structural dynamics and the actuation performances are described in detail. The effectiveness of the piezo-stack actuators in the excitation of the flexural bending modes of the structure by means of adaptive in-plane and eccentric dynamic forces is experimentally investigated. An experimental modal analysis is carried out to determine both single partition and coupled fluid-structure modal frequencies used to validate the finite element model. For the purpose of estimating the sound radiation characteristics of the window prototype, a numerical procedure coupling boundary and finite element methods will be detailed in the second part of this paper (Part 2) to solve the coupled acoustic-structure problem in the exterior acoustic domain.

Key words: structural acoustics, piezoelectric actuation, passenger comfort

1. Introduction

The importance of a quiet aircraft cabin is well documented in a number of papers dealing with the passive and active control of the cabin environment. Modern interior noise control technologies target weight-efficient solutions to improve comfort of next-generation aircrafts minimizing the effect on performances.

Although currently no certification requirement exists to regulate cabin noise levels in aircraft, comfort is particularly appreciated by end-consumers considering the effect of combined sound and vibration on comfort perception as one of the most important aircraft quality indicators (Mellert *et al.*, 2004). The dynamics of fuselage structure and the properties of the interior acoustic space are the main factors affecting the passenger's psychoacoustic response.

The existing conflict between lightweight design on the one hand and passive safety and comfort requirements on the other hand can be solved through the use of active noise reduction concepts based on intelligent materials. The integration of additional functionalities with respect to noise control can be achieved by combining conventional structures with intelligent systems, extending structural properties to sensing and actuating capabilities. A smart structure incorporates sensors and actuators in such a way that enables the structure to sense its environment and then respond adaptively.

Aircraft windows represent a significant path for structure-borne and air-borne noise transmission in the aircraft. Turbulent Boundary Layer noise is mainly transmitted into the cabin by airborne paths, but structure-borne noise, associated with engine vibrations, and the interaction between aerodynamic wakes and aircraft structure, makes a significant contribution to interior noise levels, especially at certain discrete frequencies.

Theoretical studies (David and Guillaumie, 2000; Hayde *et al.*, 1983; Röder *et al.*, 2006; Unruh and Till, 2002; Vaicaitis, 1983) indicate that the noise transmitted through windows is a predominant cause of high interior noise levels in a treated aircraft. Experiments (Guillaumie *et al.*, 2000; Hald *et al.*, 2008; Morkholt *et al.*, 2009) confirm that the airplane fuselage sidewalls in general and the passenger windows in particular, are the dominant entry path of external noise. Fuselage sidewalls radiate sound because of external forcing, causing the surface to vibrate, and absorb energy from the incident noise field because of the finite surface acoustic impedance. The distinction between the incident and the radiated field is not obvious, even in the near field, and recently novel beam-forming techniques have been proposed to enhance the spatial resolution and separate different sound field components (Morkholt *et al.*, 2009).

For a prescribed noise source, active noise control methodologies are typically categorized depending on the anti-noise strategies adopted for the interior noise reduction: at the location of noise reception or at the origin of radiation. The first approach is the loudspeaker-based active noise control (ANC), which consists of anti-noise sources, radiating a secondary noise field, able to mitigate passenger's noise reception (Tiseo *et al.*, 2007). Loudspeakers can be placed either inside the receiving enclosure (room control) or inside the cavity between the layers of double-leaf or triple-leaf partitions (cavity control) (Jacob and Moser, 2003a,b; Jacob *et al.*, 2004). The error microphones are distributed throughout the cabin space.

The other approach is the active structural acoustic control (ASAC). It aims at controlling the structural vibrations themselves by using dynamic or electric vibration absorbers (Misol and Algermissen, 2009; Yu *et al.*, 2007), properly or adaptively tuned to suppress the structure-borne noise contribution to the acoustic field. Vibration actuators and sensors, such as piezo patches, are bonded or embedded into the structure to absorb and modify vibrations, and hence the way the structure radiates noise, through their electro-mechanical coupling properties. Since each vibration mode has different radiation efficiency and some modes can be better coupled to the acoustic field than others, only few dominant radiating modes require to be controlled in amplitude. Other ASAC approaches take advantage of the acoustic radiation capabilities of the panels themselves in order to effectively control the direct sound radiation of the panel speaker so that the interior acoustic pressure is minimized.

Many airplanes use triple-pane windows, having three panes separated by air gaps, to break the vibration chain through the partitions and significantly increase the sound transmission loss. Aircraft windows can be rectangular with rounded corners, circular, elliptical or oval in shape. They cannot be square because this would cause high stress levels in the corners which can result in cracks and structural failures.

In this paper, an application-oriented approach is used to design a smart aircraft-type window prototype. The adaptive structure employs sensors, actuators and a controller to change beneficially the inherent structural characteristics in the response to an external stimulation. A multilayered partition design is used to increase the sound insulation properties. The change in density of the media travelling through the partition walls, separated by air spaces, result in a greater transmission loss than would have been provided by doubling the mass or thickness of a single partition in the same amount of space. For the purposes of this study, the window is modeled and manufactured rectangular and flat for ease of fabrication and testing. Although the obtained

results are approximately valid for a more realistic rectangular shape with rounded corners, this assumption allows one to use some analytical solutions in order to validate the numerical results. The effects of bending waves can be accurately predicted as well as the motion and forces transmitted by the control actuators. Moreover, the sound insulation properties of the triple-wall window can be predicted by using analytical models of sound transmission through finite aeroelastic multilayered partitions which assume that flat rectangular panels are acoustically coupled and simply supported in an infinite baffle.

The geometry and physical characteristics of the window prototype are therefore intended to be representative of an actual aircraft window. Firstly, the smart actuator configuration is evaluated by characterizing its effectiveness in exciting the structure at low-medium frequencies. The structural resonances are computed for the single pane and the triple pane configuration, including the modeling of the fluid between the two panes. A surface-based contact approach is used to couple the structure with the inner air. An experimental modal analysis is carried out in order to validate FE predictions. The experiments demonstrate that the elastomeric strips supporting the panes of the prototype are closely approximated by simply supported conditions. In Part 2 of this paper, the validated modal model of the structure is employed to provide an accurate estimate of the modal acoustic power and radiation efficiency for selected modes. Coincidence phenomena at which the speed of incident acoustic waves matches that of the structural bending waves are addressed. At this specific frequency and above, the acoustic waves are particularly effective in causing the structure to vibrate, making the vibrating structure a pure sound radiator whose the overall radiation efficiency is dramatically increased. However, the potential of using smart windows to control aircraft interior noise control is investigated at low frequencies where the propagation velocity of the bending wave of isotropic plates is much less of the sound speed in air. At those frequencies, coupled structural-acoustical resonances together with mass-air-mass phenomena result in a substantial decrease in the low-frequency transmission loss which can be compensated by means of active structural acoustic control.

2. The actively controlled aircraft-type window prototype

In general, airplane fuselage is composed of a structure of circular rings (frames) and longitudinal stringers on which an aluminium skin of thickness varying between 1 and 1.5 mm is wrapped. The fuselage interior is furnished by

trim panels fixed on the frames via rubber mounts. The space between the fuselage skin and the trim panels is filled with blankets of insulating material. The main purpose of this cavity treatment is thermal insulation; however, acoustic absorption is also achieved at relatively high frequencies.

The growing attention of aircraft manufacturers towards passenger comfort has accentuated the demand of novel solutions able to improve interior vibro-acoustic properties of aeronautical vehicles. Since visco-elastic damping treatments, used to reduce noise radiation on floors, sidewalls and ceilings, are not applicable for window surfaces, Fig. 1, aircraft windows represent a straightforward path by which the incoming sound energy enters the cabin. This is confirmed by high variability of the sound pressure levels existing near aircraft windows and usually being the highest at most frequencies.

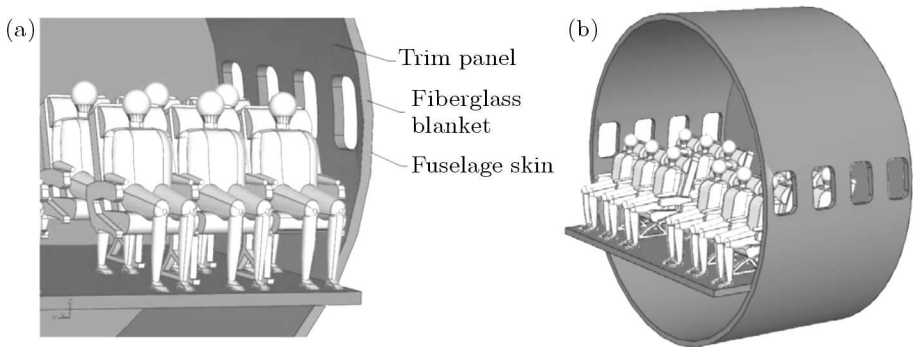


Fig. 1. Cross section of the fuselage structure

The conventional approach for determining the sound transmission properties of flat or curved structures is to mount the test article between two test chambers, typically a reverberant and an anechoic room constructed so that the only significant sound path is through the specimen, introduce sound in one of them and then measure the loss in sound power due to transmission through the specimen.

Transmission Loss tests on damped aircraft windows have demonstrated that the total sound intensity is mainly radiated by the window area and partially absorbed by the trim panel (Buehrle *et al.*, 2002, 2003, 2004). Consequently, heavy sidewall treatments, typically located behind the sidewall trim panels to attenuate noise and vibration, do not ensure an effective solution for cabin noise reduction if the windows provide a weak link in noise transmission.

The introduction of active systems on window panels can lead to a significant reduction in the transmitted noise, contributing to minimize SPL inside the cabin without affecting structural design and weight. Active noise control

systems applied to conventional homogeneous windows have been proposed in Bein *et al.* (2007), Bös *et al.* (2009), Grassi *et al.* (2007), 2003. The use of piezoceramic materials to produce control forces and bending actuation moments or to add electromechanical damping has been extensively studied in Crawley and Luis (1987), Hambric *et al.* (2006). Enabling the self-actuation and self-sensing capabilities in a structure through piezoelectric actuators, labels the structure as an adaptive structure since it is capable to control and adapt its mechanical response.

While designing smart structures for noise and vibration control, the selection of a suitable control concept is strictly related to the specific problem to be addressed. Both active vibration and noise control (AVC/ANC) and active structural acoustic control (ASAC) aim at controlling the vibro-acoustic behavior of the structural components either by minimizing the total sound power radiation or the vibrational energy using either active mounts or control loudspeakers. In the attempt to minimize the acoustic radiation, a reduction in the vibrational energy of the structure by cancelling the out-of-plane velocities does not necessary guarantee a reduction in the total sound power radiated. This is because the action of the control forces could, in principle, excite some modes, previously unexcited, which could possibly be more efficient radiators of sound. The effect is that the total sound power output could be greater than in the absence of control. Therefore, active noise control can target the cancellation of acoustic pressure at fixed points only by using control loudspeakers emitting destructive sound waves or active mounts driven by acoustic cost functions. A way to control actively noise in an enclosure consists in trying to minimize the whole acoustic potential energy (Nelson and Elliot, 1992). This potential is proportional to the volume integral of the sound pressure mean square value. The sound pressure at low frequency can be represented by a combination of a number of acoustic modes. A good estimate of the acoustic potential energy in the enclosure could be the sum of the mean square pressures measured at many different points in the room.

In this paper, a smart aircraft-type window prototype is presented. The adaptive structural system is built from a conventional triple pane window configuration, adding a number of piezoelectric stacks ensuring actuating and sensing capabilities. An ASAC strategy is implemented in order to reduce propeller-induced noise in a turboprop aircraft cabin. The structural vibrations are controlled so that the sound radiated to the environment is reduced. The active mount, studied in this paper, is based on piezo actuators, distributed along the window frame, in order to generate in-plane and eccentric forces controlling the inner plexiglas window partition. They consist of a stack of

thin ceramic disks separated by electrodes. The electro-mechanical coupling properties, describing the conversion of electric energy into mechanical energy and vice versa, are such that the piezoelectric constant d_{33} dominates the other coefficients in the constitutive equations. Unlike the laminar design where the useful direction of expansion is normal to that of the electric field, depending on d_{31} and d_{32} coefficients, these actuators are characterized by the fact that the polarization axis and the applied electric field coincide with the direction of expansion of the piezoelectric stack (IEEE, 1978). Due to high strain constants in the direction of the applied voltage, they are the most efficient piezoelectric actuators to provide high normal forces suitable for active noise and control systems.

2.1. Structural-acoustic modelling

Figure 2 shows a schematic description of the triple-glazed window. The distance between the panes are d_1 and d_2 , respectively. The velocity distributions on the panes are denoted with $v_1(x, y)$, $v_2(x, y)$ and $v_3(x, y)$, respectively from the side of sound incidence to the side of sound radiation. The sound field between pane 1 and 2 is given by $p_{12}(x, y)$ and, the sound field between pane 2 and 3 is given by $p_{23}(x, y)$.

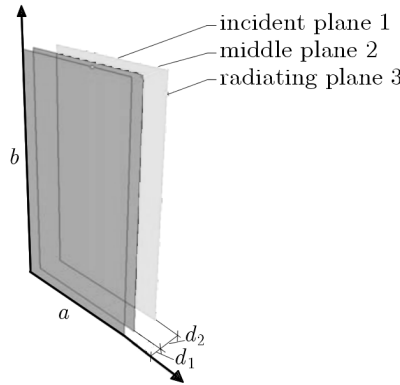


Fig. 2. Schematic of the model of the actively controlled triple-pane window

Five differential equations can be stated describing the vibrational behavior of the triple-glazed window (Jacob *et al.*, 2004)

$$\Delta \Delta v_1(x, y) - k_{B1}^4 v_1(x, y) = \frac{jk_{B1}^4}{m_1''\omega} (p_1(x, y, z = 0) - p_{12}(x, y))$$

$$\Delta p_{12}(x, y) + k_0^2 p_{12}(x, y) = \frac{j\omega\rho}{d_1} (v_2(x, y) - v_1(x, y))$$

$$\Delta \Delta v_2(x, y) - k_{B2}^4 v_2(x, y) = \frac{jk_{B2}^4}{m_2''\omega} (p_{12}(x, y) - p_{23}(x, y)) \quad (2.1)$$

$$\Delta p_{23}(x, y) + k_0^2 p_{23}(x, y) = \frac{j\omega\rho}{d_2} (v_3(x, y) - v_2(x, y))$$

$$\Delta \Delta v_3(x, y) - k_{B3}^4 v_3(x, y) = \frac{jk_{B3}^4}{m_3''\omega} (p_{23}(x, y) - p_3(x, y, z = d_1 + d_2))$$

Equations (2.1)_{1,3,5} are bending wave differential equations describing the velocity distributions of the panes. Equations (2.1)_{2,4} are differential equations for sound in the air describing the cavity sound field distributions between the three panes. Each cavity sound field is excited by the vibration of its two adjacent panes, i.e. the cavity between pane 1 and 2 (Eq. (2.1)₂) is excited by the velocity distributions $v_1(x, y)$ and $v_2(x, y)$.

In Eq. (2.1)₁, $p_1(x, y, z = 0)$ is the sound field distribution on incident pane 1 due to the incoming wave. In Eq. (2.1)₅, $p_3(x, y, z = d_1 + d_2)$ is the external sound pressure reacting on the radiating pane due to the radiating wave, i.e. the fluid loading. The fluid loading has a negligible effect and can be omitted. Δ is the Laplace operator $\Delta = \nabla^2$, k_0 is the free wave number in the air. The bending wave numbers of the panes are defined by

$$k_{Bu}^4 = \frac{m_u''}{B_u'} \omega^2 \quad (2.2)$$

with

$$B_u' = \frac{E_u}{1 - \nu^2} \frac{h_u^3}{12} \quad E_u = E_{0u}(1 + j\eta_u) \quad (2.3)$$

where $u = 1, 2, 3$ and $m_u'' = \rho_u h_u$ are the masses per unit area of the panes of densities ρ_u and thicknesses h_u , respectively. B_u' are the bending stiffnesses with Poisson's ratio ν and complex Young's moduli E_u taking the dissipation of the panes into account via the loss factors η_u .

By assuming the panes to be simply supported at the boundaries, the velocities can be written in the form

$$v_u(x, y) = \sum_{n=1}^{\infty} \sum_{m=1}^{\infty} V_{unm} \sin \frac{n\pi x}{a} \sin \frac{m\pi y}{b} \quad (2.4)$$

with modal amplitudes V_{unm} where $u = 1, 2, 3$.

For the cavity sound fields, the modal functions can be written in the form

$$p_w(x, y) = \sum_{p=0}^{\infty} \sum_{q=0}^{\infty} A_{wpq} \cos \frac{p\pi x}{a} \cos \frac{q\pi y}{b} \quad (2.5)$$

with modal amplitudes A_{wpq} where $w = 12, 23$.

Compared to single panels, infinite multi-pane panels generally yield a higher transmission loss, except around the low-frequency mass-air-mass resonance where the two adjacent glass plates oscillate in anti-phase against the stiffness of the compressible acoustic medium in the cavity. For a double-wall partition, the mass-air-mass resonance is defined as

$$\omega_0 = \sqrt{\frac{\rho_0 c_0^2}{L_c^z} \left(\frac{m_{p1} + m_{p2}}{m_{p1} m_{p2}} \right)} \quad (2.6)$$

where L_c^z is the distance between two panes, ρ_0 the density of the acoustic medium in the cavity (1.225 kg/m^3), c_0 the sound speed in that medium (340 m/s), and m_{p1} and m_{p2} represent the mass per unit area of both plates.

2.2. The window design

Despite the acoustic transmission characteristics of aircraft-type windows have been extensively studied for single and double pane configurations (Hills *et al.*, 2006; Navaneethan *et al.*, 1980; Rassaian *et al.*, 2008), only few papers provide numerical and experimental data for triple pane windows. Multi-glazed windows provide good sound insulation only at relatively high frequencies. Due to the mass-air-mass resonance, their acoustic performance rapidly deteriorates at low frequencies, where the sound transmission loss can even become worse than that of a single partition. The design of the active aircraft-type window is here reported. The dynamic behavior of the triple wall system is analyzed. The low-frequency sound insulation characteristics and the sound transmission loss will be addressed in Part 2, where the benefits achieved by coupling a three-layer configuration with an adaptive control system will be also experimentally investigated.

The prototype consists of an aluminium frame, measuring $22.2 \text{ cm} \times 34.2 \text{ cm} \times 8.72 \text{ cm}$, containing three window panes with a transparent area of $32 \text{ cm} \times 20 \text{ cm}$. Two of the three panes are made of 0.94 cm thick glass and are separated by an airspace of 1.66 cm . The third pane, which is made of acrylic, is 0.64 cm thick and is separated from one of the glass pane by a 3.62 cm airspace. When the window is installed, the acrylic pane faces the inside of the fuselage cabin. The panes are supported by strips of elastomer. A silicon rubber is used to secure the windows in the aluminium frame. A sketch of the window frame and layers is shown in Fig. 3a. Figure 3b shows a section of the assembled prototype, including the layers and the strips of elastomer.

Concerning the actuation, no. 10 piezoelectric stack actuators are mounted on the sides of the window. A planar actuation system is constrained to the

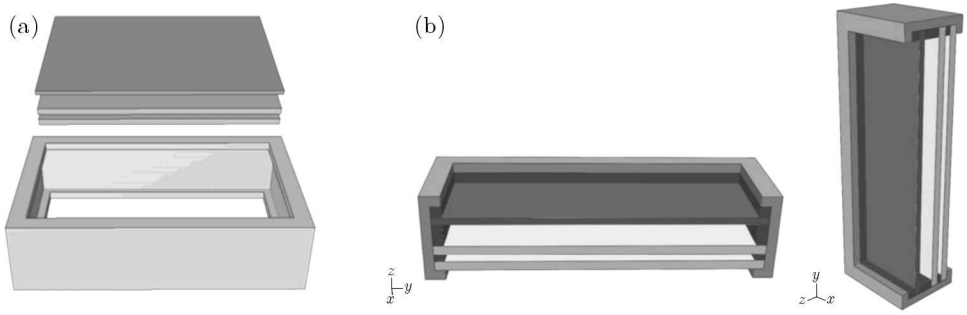


Fig. 3. (a) Window sketch. (b) Assembled prototype

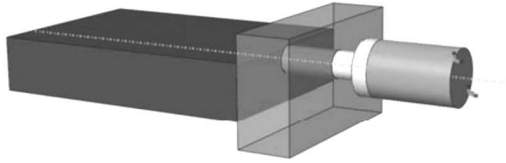


Fig. 4. Sketch of the single actuation mechanism

window frame by means of a dedicated system of clamping. Each stack is pre-stressed by the action of a screw compressing the actuator to the acrylic pane through a metal rod. A sketch of the actuator mechanism is shown in Fig. 4. In this configuration, the actuator generates an off-midplane actuation force on the active pane inducing local bending moments capable of exciting and hence controlling the transverse modes.

The manufacturing of the prototype required the machining of light-weight clamping systems constraining the piezo actuators. A sketch of the distributed piezo stacks and their clamping systems is reported in Fig. 5a. A picture of the assembled window prototype is depicted in Fig. 5b. Figure 5c shows the clamping system. The prototype has been manufactured and preliminary tested in laboratory.

2.3. Numerical modelling

A FE model of the structure has been developed to evaluate the structural dynamics. The two glass and acrylic panes, the elastomer and the aluminium frame have been individually modeled with constant material properties. They are listed in Table 1.

Two-dimensional shell elements have been used, Fig. 6. The model of the aluminium frame, the glass and plexiglas partitions and the elastomer gasket totally consist of 3344 linear quadrilateral elements of 4-node general-purpose S4 shells. The assembled FE model of the prototype is shown in Fig. 7.

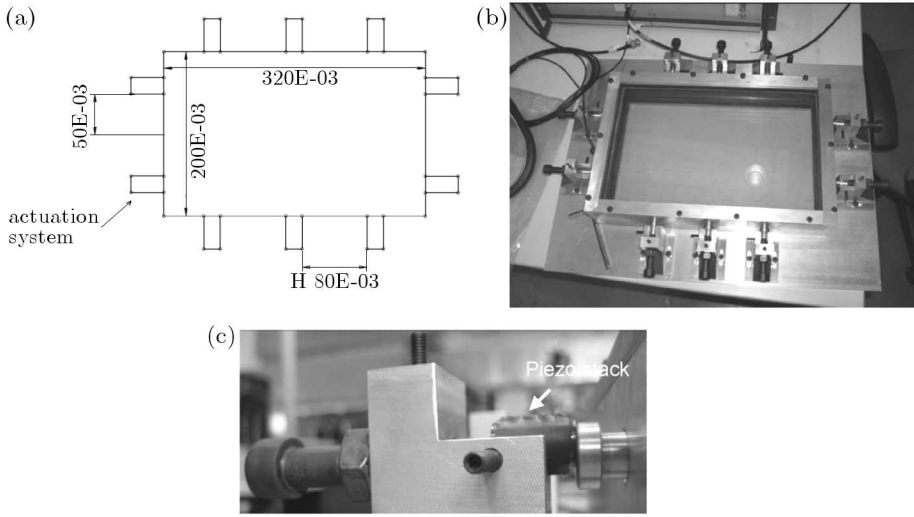


Fig. 5. (a) Sketch of the actuation grid. (b) Active window prototype. (c) Clamping system of the piezo actuators

Table 1. Material properties of the window

Material	Young's modulus [N/m ²]	Poisson's ratio [-]	Density [kg/m ³]
Plexiglas	0.31E+10	0.40	1190
Glass	6.20E+10	0.24	2480
Elastomer	2.50E+7	0.49	1300
Aluminium	7.24E+10	0.33	2780

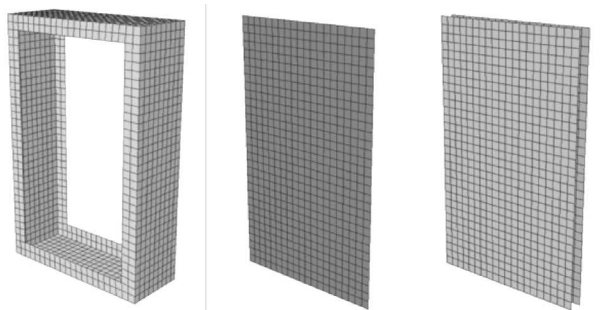


Fig. 6. Aluminium box, the plexiglas layer and the two glass layers

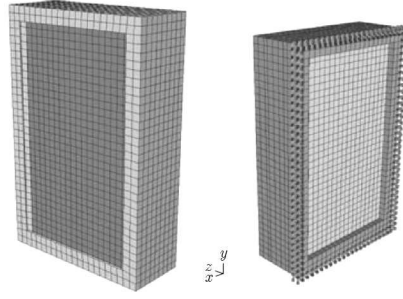


Fig. 7. FE model of the prototype

Before analyzing the whole system, the modal characteristics of each element of the window have been individually studied. The natural frequencies of the three layers of the window have been analytically calculated in simply supported boundary conditions, with

$$f_{l,n} = \frac{\pi}{2} \sqrt{\frac{Et^2}{12(1-\nu^2)\rho} \left[\left(\frac{l}{a}\right)^2 + \left(\frac{n}{b}\right)^2 \right]} \quad (2.7)$$

where t is thickness, ρ is the surface density, and a and b are the width and the length of the window panes. Such frequencies are tabulated in Table 2 and compared to the numerical resonances computed for each single-pane. A modal analysis of the assembled model has been carried out in ABAQUS. Natural frequencies and mode shapes have been computed in the frequency range up to 1 KHz. The clamped boundary conditions have been prescribed at the outer surface nodes, as described Fig. 7 (right). As shown in Table 2, a reasonable agreement between mode (1,1) and mode (1,2) of the simply-supported acrylic pane and the respective modes of the outer plexiglas layer of the window prototype, has been observed. This confirms that the boundary conditions with the panes supported by the elastomer, as described in Fig. 3b, are approximated closely by simply supported conditions. Such an assumption is also confirmed by the results reported in Grosveld (1988) for a similar triple-pane window architecture.

Being a triple-leaf partition, particular attention has been paid to the simulation of the air gap between the plexiglas and the upper glass layer and that between the upper and lower glass layers. The air between the plexiglas and the glass layer has been modeled with 2560 linear hexahedral elements of type AC3D8, while 1280 AC3D8 elements have been used to fill in the volume of the interior air between the two glass layers, Fig. 8. To simplify the problem, the effect of interacting air at the outside of the window box has been

Table 2. Calculated and measured window resonance frequencies

Resonance system	Material	Thick-ness [cm]	Mode	Calc. suply supported [Hz]	FE model [Hz]	FE model Air gap model. [Hz]	Experim. analysis		
							no comp. [Hz]	1 Nm [Hz]	2 Nm [Hz]
Single layer	Acrylic	0.64	1.1	177.58	175.77				
			1.2	327.23	324.65				
			2.1	560.69	555.15				
			1.3	576.65	570.75				
	Glass	0.94	1.1						
			1.2	1405.7	1389.3				
Window prototype			1.1		170.48	194.17	197	193	192
			1.2		304.76	297.52	264	255	251
			2.1		475.37	470.36	455	447	450
Cavity resonance						538.06	536	538	541

neglected. The air has been modeled with density of 1.225 kg/m^3 and bulk modulus of 0.142 MPa . The surface-based contact approach has been used to couple the structural and acoustic meshes. Surfaces have been defined for the frame, the two opposite layers and the free surface of the air. The TIE option has been used to couple the structure with the inside air. As a result, the numerical model could simulate the acoustic coupling effects considering the acoustic medium tied to the structure. The natural frequencies computed for the uncoupled and coupled system are given in Table 2. The uncoupled natural frequencies are also given in order to show how the structure-acoustic coupling affects the characteristics of the system.

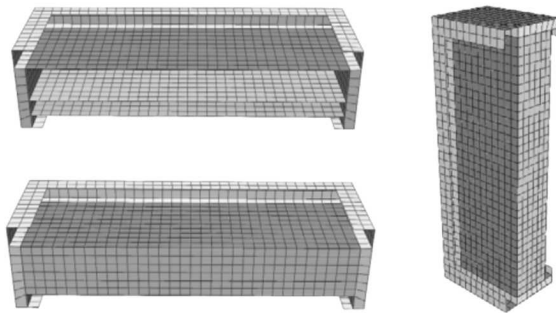


Fig. 8. Air gap modelling

Due to the coupling effects, the eigenfrequencies shifted mode by mode. The first natural frequency of the coupled system has been observed higher

than the first natural frequency of the structural model. This is because the acoustic chamber, represented by the fluid between the panes, “spring-loads” the two plates. Each mode shape exhibited also more complex behavior with respect to the structural modes, so that each mode had nonzero components on both the structural and acoustic part.

Some mode shapes computed for the uncoupled case are reported in Fig. 9.

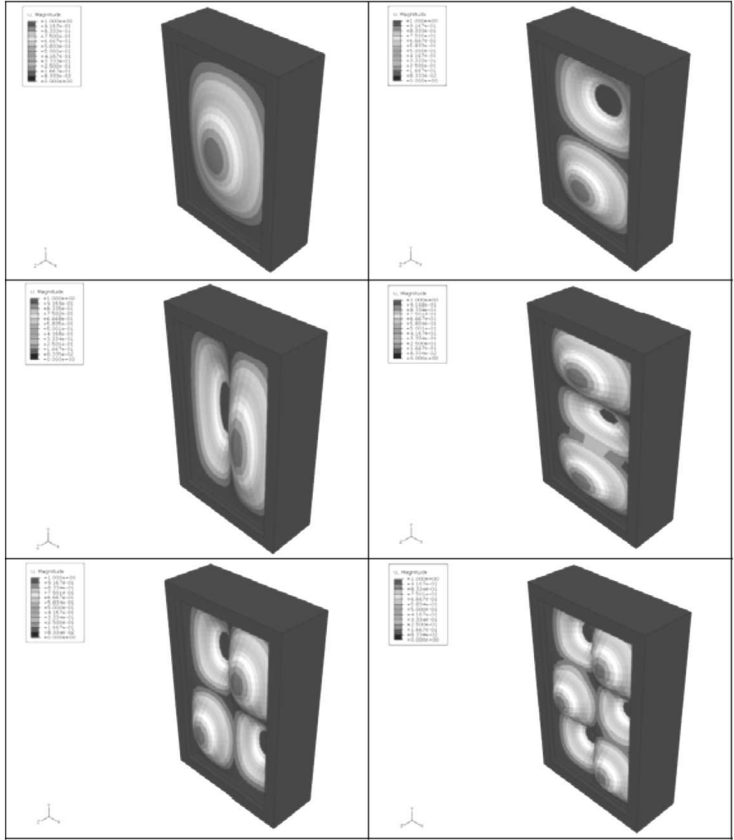


Fig. 9. Modes of the structure

The coupled structural-acoustic analysis resulted in an equal distribution of the normal velocity for both the structural and the acoustic meshes. The sound pressure distribution of the acoustic medium, due to the coupled modes, has been calculated for the interior domain. As shown in Fig. 10a, the pressure distribution in the air gap between the plexiglas and the upper glass layer (left side of the picture) matches the first bending mode (1,1) of the plexiglas plate (right side of the picture). The same behavior has been observed also for the

second bending mode (1,2), as shown in Fig. 10b. The first mode shape of the system scaled to the aluminium frame is shown in Fig. 11a. Finally, the cavity resonance occurring in the air volume comprised between the plexiglas and the upper glass layer is shown in Fig. 11b.

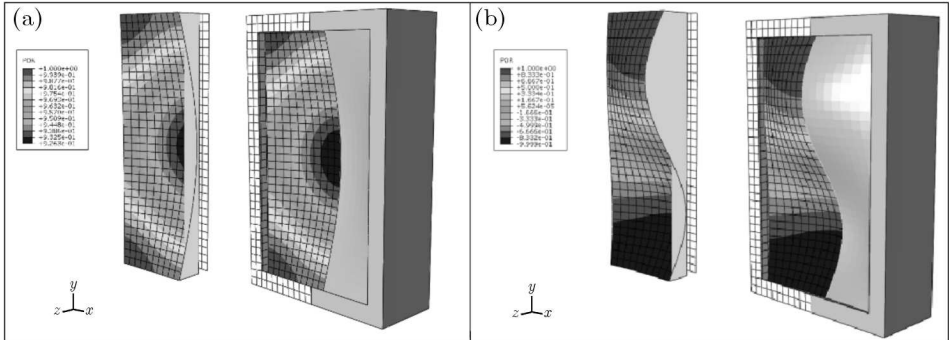


Fig. 10. Section of the pressure distribution in the air gap between the plexiglas and glass layer – 1st mode (a), 2nd mode (b)

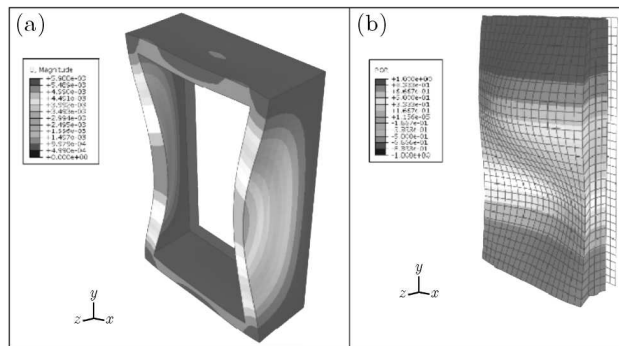


Fig. 11. (a) Frame components of the 1st mode shape. (b) Cavity resonance in the air gap between the plexiglas and glass layer

2.4. Experimental activities

An experimental modal analysis has been carried out in order to validate the FE model of the structure. The experimental set-up consisted of an instrumented hammer, used to excite the structure, and 18 accelerometers distributed on a regular mesh. Data acquisition was done with the LMS SCADAS data acquisition system. The transducers have been installed so as to minimize the effects of mass-loading due to the sensors. The structure has

been tested clamped on the reference panel resting on a block of foam rubber to simulate the free-free boundary conditions.



Fig. 12. Experimental modal tests on the window prototype

The mesh grid has been drawn on the plexiglas. The acquisition system recorded simultaneously both the force impulse generated by the hammer and the vibrations measured by the accelerometers. From the measured data, the Frequency Response Functions have been computed by using a curve fitting method in order to extract the structural modes. The modal parameters have been calculated by the LMS Polymax method. Figure 13 shows two experimental FRFs measured on point no. 5 and point no. 8 respectively, both located nearby the centre of the plexiglas plate, Fig. 16. No pre-stress through the screws has been imposed, as numerically simulated in the FE model. The first two experimental mode shapes measured on the structure are shown in Fig. 14.

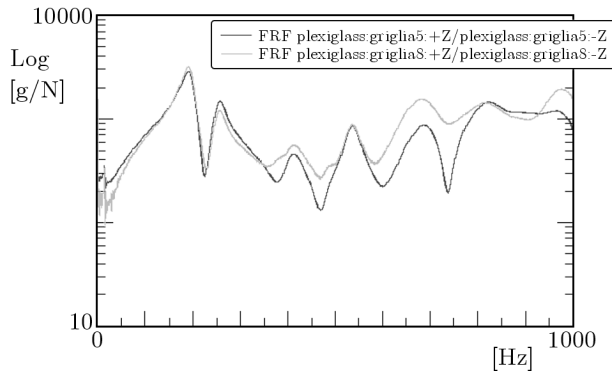


Fig. 13. Experimental FRF measured by two sensors

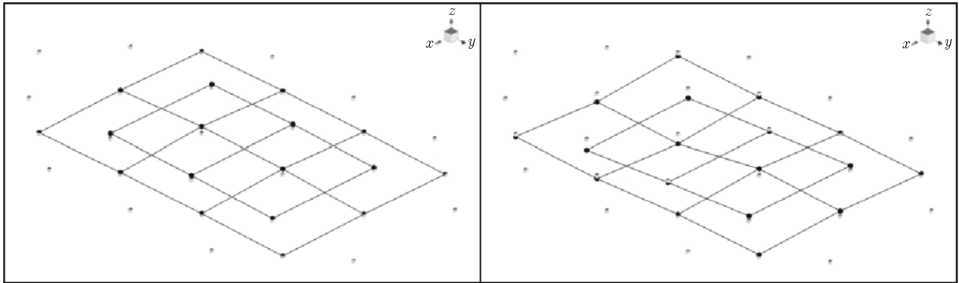


Fig. 14. Experimental mode shapes: left (1,1), right (1,2)

The experimental modal frequencies are tabulated in Table 2. A good agreement between the experimental and numerical resonances has been observed, especially for those resulting from the acoustic-structural coupled analysis.

The influence of the mechanical pre-stress onto the structure has been also examined. To this aim, a uniform torque has been applied to the screws constraining the piezo actuators through the borders. This static load determined a slight reduction in the resonance frequencies of the structure depending on the amplitude of the mechanical compressive axial force, as shown in Fig. 15. The resonance frequencies decreased with the increasing compression preload. This has been demonstrated for two different levels of torque (1 Nm, 2 Nm) tightening the screws.

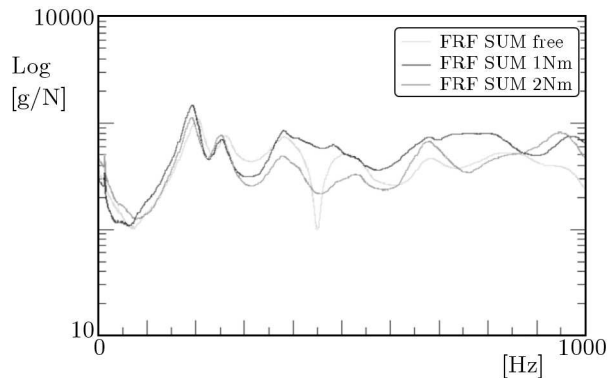


Fig. 15. Influence of the compressive preload on the structural response

A further validation of the dynamic behavior of the prototype has been carried out in operative conditions. The window has been installed on the side of a plumb steel box (2 tons of weight), used as the reference facility for the active noise control experiments described in Dimino *et al.* (2010a-c), Fig. 16. Unlike the previous experiments, the structure has been directly excited by the

piezoelectric stack actuators. The experimental set-up consisted of 12 accelerometers, a signal generator and 10 amplifiers needed to drive the piezoelectric actuators. The transfer functions of the acrylic pane have been measured by imposing a broadband sweep excitation.

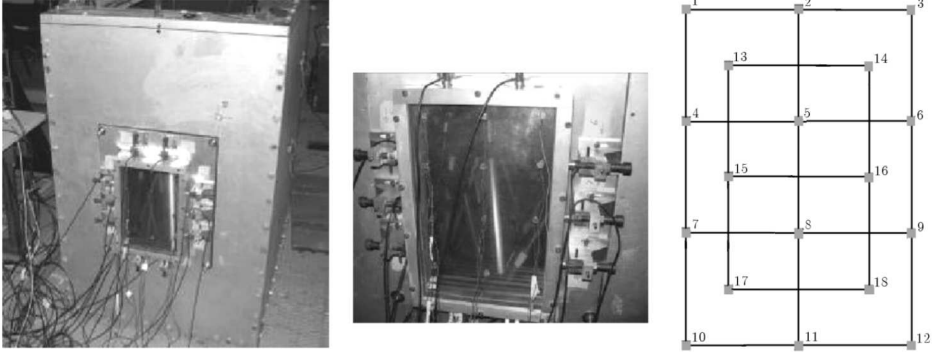


Fig. 16. Active window mounted on the acoustic facility

Different levels of excitations driving the piezo actuators have been imposed in order to capture potential non-linearities in the actuation chain in the frequency range 100-1000 Hz. The voltage has been set in the range of 100 to 400 V. In the latter configuration, a non-linear response of the actuator has been observed due to the power saturation limit. Figure 17 shows the FRFs measured by two different points for each level of excitation.

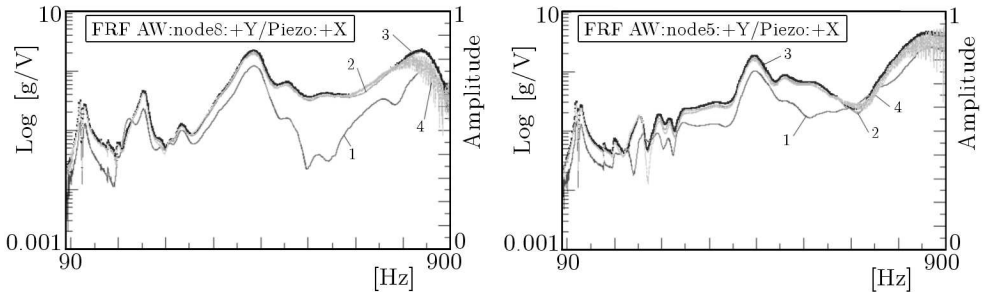


Fig. 17. FRFs measured on point 8 (left) and point 5 (right). Four input levels (1 – 100 V, 2 – 200 V, 3 – 300 V, 4 – 400 V)

Since the choice of the actuator positions represents a crucial issue in the design of smart structures, the influence of the actuation points has been investigated. In principle, the piezoelectric actuators must be placed in regions of high average strain and away from areas of zero strain (Crawley and Luis, 1987). The position of these “strain nodes” is determined by twice differentia-

ting the analytic expressions for the plate modes and finding the zero-crossing points of the resulting functions. For the second mode (1,2) of a simply supported plate, for instance, the actuators located behind such strain nodes must be driven 180 deg out of phase with respect to the piezo located ahead. This means that it is necessary to control individually the driving voltage applied to each actuator in order to control each flexural mode effectively. This cannot be done if the actuators are continuous over the length of the structure. For these reasons, segmented actuators are normally preferred in the control of flexible structures.

Figures 18 and 19 describe the experimental FRFs obtained by exciting the structure by single or grouped piezo stacks. Each color identifies both the piezo actuator and the respective FRF. As expected, the simultaneous control of eight piezo stacks (8 input channels) determined a good excitation of all the structural modes included in the frequency range of interest, (b curve), with particular reference to the symmetric modes. Obviously, such a condition cannot be considered as an optimal configuration since it has been obtained by equally controlling each actuator. For this reason, further improvements can be achieved by optimizing amplitude and phase signals driving each actuator.

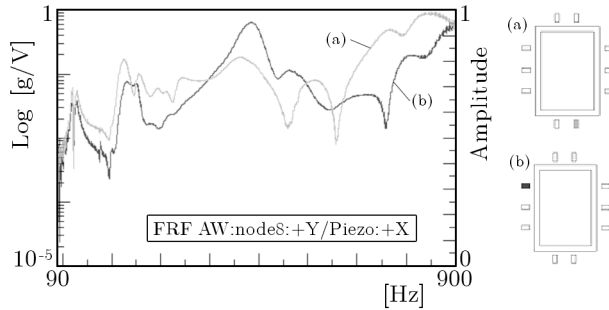


Fig. 18. Influence of the actuation point on the experimental FRFs

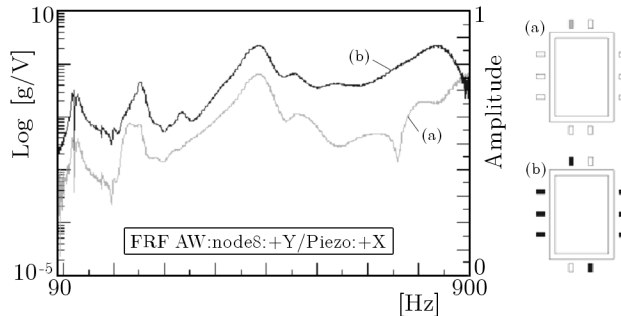


Fig. 19. Influence of the actuation point on the experimental FRFs

Finally, the acoustic radiation properties of the window have been investigated in anechoic conditions, Fig. 20. A microphone has been installed inside an anechoic chamber at a distance of 1 m from the window prototype. The piezoelectric actuators have been excited in the frequency range of 200-2000 Hz. A voltage transformer allowed achieving the high voltage required to drive the actuators. The output of the pressure transducer has been sampled and processed with a spectrum analyzer. Figure 21 shows the experimental Frequency Response Function of the acoustic pressure measured by the microphone. Such a curve, generally flat for a commercial loudspeaker, provides a basic understanding of the acoustic radiation of a flexible structure. From this preliminary analysis, it can be noted that the acoustic radiation of the structure exhibited antiresonances in the regions between 700-1000 Hz and 1800-2000 Hz. A more detailed analysis of the structural radiation efficiency in the low-medium frequency range will be addressed in Part 2 of this paper. Such a study impacts also the design of an active noise control system suitable for the interior noise control of a turbo-prop aircraft (Dimino *et al.*, 2010c).

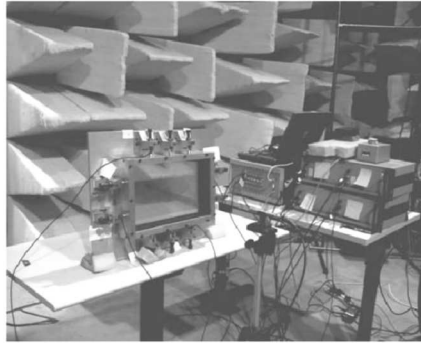


Fig. 20. Acoustic measurements in the anechoic chamber

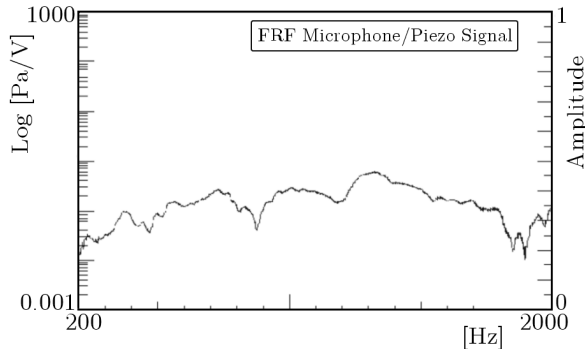


Fig. 21. Acoustic FRF of the widow prototype

3. Conclusions

Next generation aircraft will have larger windows and composite fuselages. For this reason, the window design must be optimized to provide maximum passenger external visibility while minimizing acoustic noise transmitted through the windows. This paper is the first part of two companion papers. In this part, the design of a smart aircraft-type window prototype is presented. Such an adaptive structure is built from a passive, conventional, triple pane window adding a number of piezo stacks controlling the structural panes. The main benefits are related to the coupling between the enhanced sound transmission loss due to the multi-partition design, and the active control aptitudes provided by the piezo actuators.

The actuation mechanism, based on piezo-induced vibrations exciting the structural flexural modes, has been experimentally validated. For a proper installation of the actuators, a mechanical preload has been required to compensate the small extensional strength of the stacks so that the piezo-induced strains resulted smaller than the mechanical strains imposed through the compressive preloads. The vibro-acoustic properties of the window prototype have been numerically and experimentally investigated. The structural frequencies of resonance have been computed for the single pane individually as well as for the whole system, including the modeling of the fluid between the panes. An experimental modal analysis has been carried out to validate the FE model. Experiments have demonstrated that the elastomeric strips supporting the panes of the prototype can be well approximated by simply supported conditions. Due to the fluid-structure coupling effect, the eigenfrequencies shifted mode by mode. The first natural frequency of the coupled system resulted larger than the first natural frequency of the structure due to the interaction between the fluid and the flexible structure. The sound pressure distribution has been calculated in the interior domain. The link between the kinetic energy of the vibrating structure and the acoustic emission properties of the structural modes will be discussed in Part 2 of this paper.

Acknowledgments

The content of this paper is part of a research project funded by CIRA (The Italian Aerospace Research Centre) and the Campania Region, Italy. The authors would like to acknowledge the experimental support of the Centre for Acoustics and Vibration (CAV) of Penn State University, Pennsylvania, USA.

References

1. BEIN T., DOLL T., KURTZE L., 2007, Active facades to reduce noise emissions, *Intelligent Glass Solutions*, **3**, 41-44
2. BÖS J., HEROLD S., HEUSS O., KAUBA M., MAYER D., 2009, Active control of the sound transmission through a double-glazing window, *Proceedings NAG/DAGA 2009*, Rotterdam, 1224-1227
3. BUEHRLE R., GIBBS G., KLOS J., 2004, Damped windows for aircraft interior noise control, *NOISE-CON 2004*
4. BUEHRLE R., GIBBS G., KLOS J., MAZUR M., 2003, Modeling and validation of damped plexiglas windows for noise control, *NASA Technical Report*, Document ID: 20040085762
5. BUEHRLE R., GIBBS G., KLOS J., SHERILYN A., 2002, Noise transmission characteristics of damped plexiglas windows, *NASA Langley Research Center, 8th AIAA/CEAS Aeroacoustics Conference*
6. CRAWLEY E.F., DE LUIS J., 1987, Use of piezoelectric actuators as elements of intelligent structures, *AIAA Journal*, **25**, 10, 1373-1385
7. DAVID J.M., GUILLAUMIE L., 2000, Vibration and internal noise prediction of an aircraft fuselage in the low and medium frequency ranges, *ISMA 25 Conference*, Leuven, Belgium
8. DE GRASSI M., NATICCHIA B., CARBONARI A., 2007, Design and development of an active controlled window with high sound transmission loss, *24th International Symposium on Automation and Robotics in Construction (ISARC 2007)*
9. DIMINO I., CONCILIO A., ALIABADI M.H., PIERRÈ A., 2010a, A feedforward control system for the active noise control of a triple-pane aircraft-type window, *17th International Congress on Sound and Vibration, ICSV17 2010*, Cairo Egypt
10. DIMINO I., CONCILIO A., ALIABADI M.H., PIERRÈ A., 2010b, Active noise control using DSP: experimental activities on advanced aircraft windows, *21st International Conference on Adaptive Structures and Technologies (ICAST 2010)*, Penn State University, Pennsylvania
11. DIMINO I., CONCILIO A., ALIABADI M.H., PIERRÈ A., 2010c, Modeling of an active interior noise control system for advanced aircraft windows, Submitted to *AIAA Journal of Aircraft*
12. GROSVELD F.W., 1988, Acoustic transmissibility of advanced turboprop aircraft windows, *Journal of Aircraft*, **25**, 8
13. GUILLAUMIE L., DAVID J.M., VOISIN-GRALL O., 2000, Internal fuselage noise: comparison of computations and tests on a Falcon airframe, *J. Aerospace Science and Technology*, **4**, 8, 545-554

14. HALD J., MØRKHOLT J., HARDY P., TRENTIN D., BACH-ANDERSEN M., KEITH G., 2008, *Array Based Measurement of Radiated and Absorbed Sound intensity Components*, Dissemination of the CREDO project, "Cabin noise Reduction by Experimental and numerical Design Optimization", Acoustics
15. HAMBRIC S.A., FAHNLIN J.B., KANKEY A.T., KOOPMANN G.H., 2006, Proposed piezoceramic excitation for translational and rotational mobility measurements, *Noise Control Engineering Journal*, **54**, 4
16. HAYDEN R.E., MURRAY B.S., THEOBALD M.A., 1983, *A Study of Interior Noise Levels, Noise Sources and Transmission Paths in Light Aircraft*, NASA CR-172152
17. HILLS K., WONG S., PARE M., MILLER W., WAIDNER NOVAK K., MUMM R., 2006, *Integrated Window Belt System for Aircraft Cabins*, United States Patent, No. US 7,118,069 B2, Oct. 10
18. IEEE 1978, *Piezoelectricity IEEE Standard 176*, New York: IEEE
19. JACOB A., BAUERS R., MOSER M., 2004, An actively controlled triple-glazed window, *Internoise 2004*, Prague
20. JACOB A., MOSER M., 2003a, Active control of double-glazed windows. Part I: Feedforward control, *Applied Acoustics*, **64**, 2, 163-182
21. JACOB A., MOSER M., 2003b, Active control of double-glazed windows. Part II: Feedback control, *Applied Acoustics*, **64**, 2, 183-196
22. MELLERT V., BAUMANN I., FREESE N., WEBER R., 2004, Investigation of noise and vibration impact on aircraft crew, studied in an aircraft simulator, *Inter Noise 2004*, Prague, ISBN: 5-7325-0816-3, 8 pages
23. MISOL M., ALGERMISSEN S., 2009, Reduction of interior noise in an automobile passenger compartment by means of active structural acoustic control (ASAC), *Proceedings of NAG/DAGA 2009*, Rotterdam, Nederlande
24. MØRKHOLT J., HALD J., HARDY P., TRENTIN D., BACH-ANDERSEN M., KEITH G., 2009, Measurement of absorption coefficient, surface admittance, radiated intensity and absorbed intensity on the panels of a vehicle cabin using a dual layer array with integrated position measurement, *SAE International Journal of Passenger Cars – Mechanical Systems*, **2**, 1449-1457
25. NAVANEETHAN R., GROSVELD F., ROSKAM J., 1980, Noise reduction characteristics of general aviation type dual pane windows, *AIAA Paper*, 80-1874
26. NELSON P.A., ELLIOT S.J., 1992, *Active Control of Sound*, New York: Academic Press
27. RASSAIAN M. ET AL., 2008, *Optimal Aircraft Window Shape for Noise Control*, US Patent NO. US7438263B2, Oct. 21, Assignee: The Boeing Company
28. RÖDER ?, PEIFFER A. AND EU PARTNERS, 2006, Deliverable DWP1.1 *Definition of the Acoustic Environment in Typical Aircraft and Helicopter Cabin*, EU-Project CREDO, Project Nr. AST5-CT-2006-030814

29. TISEO B., DIMINO I., GIANVITO A., CONCILIO A., 2007, A broadband acoustic feedback control system on confined area on board of aircraft, *13th AIAA/CEAS Aeroacoustics Conference*, Rome, Italy
30. UNRUH J.F., TILL P.D., 2002, *General Aviation Interior Noise: Part III – Noise Control Measure Evaluation*, NASA Technical Report, NASA/CR-2002-211667
31. VAICAITIS R., 1983, *Study of Noise Transmission Through Double Wall Aircraft Windows*, NASA Technical Report, NASA CR 172182
32. YU X., ZHU H., RAJAMANI R., STELSON K.A., 2007, Acoustic transmission control using active panels: an experimental study of its limitations and possibilities, *Smart Materials and Structures*, **16**, 2006-2014

Projekt profilu wibroakustycznego aktywnego okna lotniczego. Część 1: modelowanie dynamiczne i weryfikacja doświadczalna

Streszczenie

Ostatnio przeprowadzone badania pokazały, że skuteczność aktywnych metod redukcji hałasu stosowanych w oknach montowanych w samolotach można podnieść w zakresie niskich częstotliwości. Wobec szczególnie korzystnych warunków transmisji zewnętrznego hałasu w samolocie i jego wysokiego poziomu, odpowiedni projekt okna lotniczego może znacząco przyczynić się do ograniczenia hałasu w kabinie, przy minimalnej ingerencji w masę i osiągi samolotu. Prezentowany artykuł stanowi pierwszą część podwójnej publikacji na omawiany temat. W tej części opisano projekt profilu wibroakustycznego prototypu trójszybowego okna lotniczego. Bardzo szczegółowo przedstawiono numeryczne i doświadczalne aspekty badań mających na celu określenie dynamiki układu oraz wydolności aktywnego sterowania. Stosując adaptacyjny, płaski i mimośrodowy układ przykładanych sił, przeprowadzono badania eksperymentalne nad skutecznością piezoelektrycznych elementów wykonawczych w tłumieniu giętych postaci drgań okna. Dla weryfikacji modelu elementów skończonych dokonano także doświadczalnej analizy modalnej, co pozwoliło na wyznaczenie częstości własnych pojedynczej struktury oraz układu ze sprzężeniem poprzez oddziaływanie z płynem. W części drugiej oszacowane zostaną charakterystyki radiacji dźwięku w prototypie okna. W tym celu użyta będzie procedura łącząca metodę elementów brzegowych i skończonych, która umożliwi rozwiązanie sprzężonego, akustyczno-strukturalnego problemu emisji hałasu w zewnętrznym obszarze akustycznym.

Manuscript received November 19, 2010; accepted for print May 13, 2011